AGU PUBLICATIONS

Geophysical Research Letters

RESEARCH LETTER
10.1002/2016GL071538

Key Points:
- Radar reflectivity shows extensive wintertime subglacial water storage primarily on basal ridges in Greenland
- In the summertime, reflectivity data show that the drainage pattern changes with deep troughs conduct water when the ridges drain
- Seasonal changes in subglacial drainage distribution are controlled by the material properties of the glacier bed

Supporting Information:
- Supporting Information S1

Correspondence to:
W. Chu,
wchu@ldeo.columbia.edu

Citation:
Chu, W., D. M. Schroeder, H. Seroussi, T. T. Creyts, S. J. Palmer, and R. E. Bell (2016), Extensive winter subglacial water storage beneath the Greenland Ice Sheet, *Geophys. Res. Lett.*, *43*, 12,484–12,492, doi:10.1002/2016GL071538.

Received 18 OCT 2016
Accepted 8 DEC 2016
Accepted article online 9 DEC 2016
Published online 29 DEC 2016

Extensive winter subglacial water storage beneath the Greenland Ice Sheet

Winnie Chu[1], Dustin M. Schroeder[2], Helene Seroussi[3], Timothy T. Creyts[1], Steven J. Palmer[4], and Robin E. Bell[1]

[1]Lamont-Doherty Earth Observatory, Columbia University, Palisades, New York, USA, [2]Department of Geophysics, School of Earth, Energy and Environmental Sciences, Stanford University, Stanford, California, USA, [3]Jet Propulsion Laboratory, California Institute of Technology, Pasadena, California, USA, [4]College of Life and Environmental Sciences, University of Exeter, Exeter, UK

Abstract Surface meltwater that reaches the base of the Greenland Ice Sheet exerts a fundamental impact on ice flow, but observations of catchment-wide movement and distribution of subglacial water remain limited. Using radar-sounding data from two seasons, we identify the seasonal distribution of subglacial water in western Greenland. Our analysis provides evidence of widespread subglacial water storage beneath Greenland in the wintertime. The winter storage is located primarily on bedrock ridges with higher bed elevations in excess of 200 m. During the melt season water moves to the subglacial troughs. This inverse relationship with topography indicates that the material properties of the glacier bed strongly influence subglacial drainage development. Both the spatial variations in bed properties and the initial state of the subglacial hydrology system at the start of the melt season lead to differing glacier dynamical responses to surface melting across the Greenland Ice Sheet.

1. Introduction

The contribution of the Greenland Ice Sheet to sea level rise has doubled in the last decade, with a significant contribution from increased melting on the ice sheet surface [*Rignot and Kanagaratnam*, 2006; *van den Broeke et al.*, 2009]. When this surface meltwater reaches the bed, it lubricates the interfaces and can cause a transient increase in glacier speed [*Alley et al.*, 2005; *McMillan et al.*, 2007; *Das et al.*, 2008; *Smith et al.*, 2015]. The seasonal transition in subglacial drainage controls the coupling between surface melting and ice motion [*Zwally et al.*, 2002; *Schoof*, 2010; *Bartholomew et al.*, 2011; *Palmer et al.*, 2011; *Sundal et al.*, 2011; *Andrews et al.*, 2014]. In winter, when the supply of meltwater is low, drainage pathways close and the system is poorly connected [e.g., *Bartholomew et al.*, 2012; *Hewitt*, 2013]. During the melt season, the supply of surface water to the bed increases the connectivity of the drainage system. This addition of water at the bed increases water pressures until the capacity of the drainage system increases to accommodate the additional water input [e.g., *Schoof*, 2010; *Sundal et al.*, 2011; *Tedstone et al.*, 2013]. Competing effects of sliding, variations in meltwater input, and evolution of the subglacial drainage system cause variations in speed through the melt season. The exact effects of surface melt are not well understood, but the system is widely viewed as hysteretic with spring and summer water input yielding increased sliding to a threshold [*Iken and Bindschadler*, 1986; *Schoof*, 2005]. Once that input threshold is reached, an increase in water input leads to a decrease in sliding during late summer and the transition into fall and winter [*Sole et al.*, 2013; *Tedstone et al.*, 2013].

In Greenland, this seasonal melt supply produces complex velocity changes with strong variability at scales of tens of kilometers. Within individual catchments, seasonal glacier speedups range from 10% to over 300% above the winter speeds [*Zwally et al.*, 2002; *Palmer et al.*, 2011; *Joughin et al.*, 2013; *Andrews et al.*, 2014]. Across Greenland, individual glaciers also show substantially different responses for similar surface melt production and climate forcing [*Joughin et al.*, 2010; *Fitzpatrick et al.*, 2013; *Moon et al.*, 2014]. Part of this complexity is governed by the spatial distribution of moulins and supraglacial lakes [*Joughin et al.*, 2013; *Smith et al.*, 2015]. However, when this meltwater reaches the bed, seasonal changes in basal water pressures can reroute its flow paths subglacially across neighboring catchments [*Lindbäck et al.*, 2015; *Chu et al.*, 2016]. Catchment-scale observations of subglacial drainage are necessary to establish the spatial linkage between surface melt, subglacial drainage, and ice velocity.

Ice-penetrating radar is a powerful technique for catchment-scale detection of subglacial water bodies. Higher radar bed reflectivity can indicate subglacial water as water produces a stronger dielectric contrast

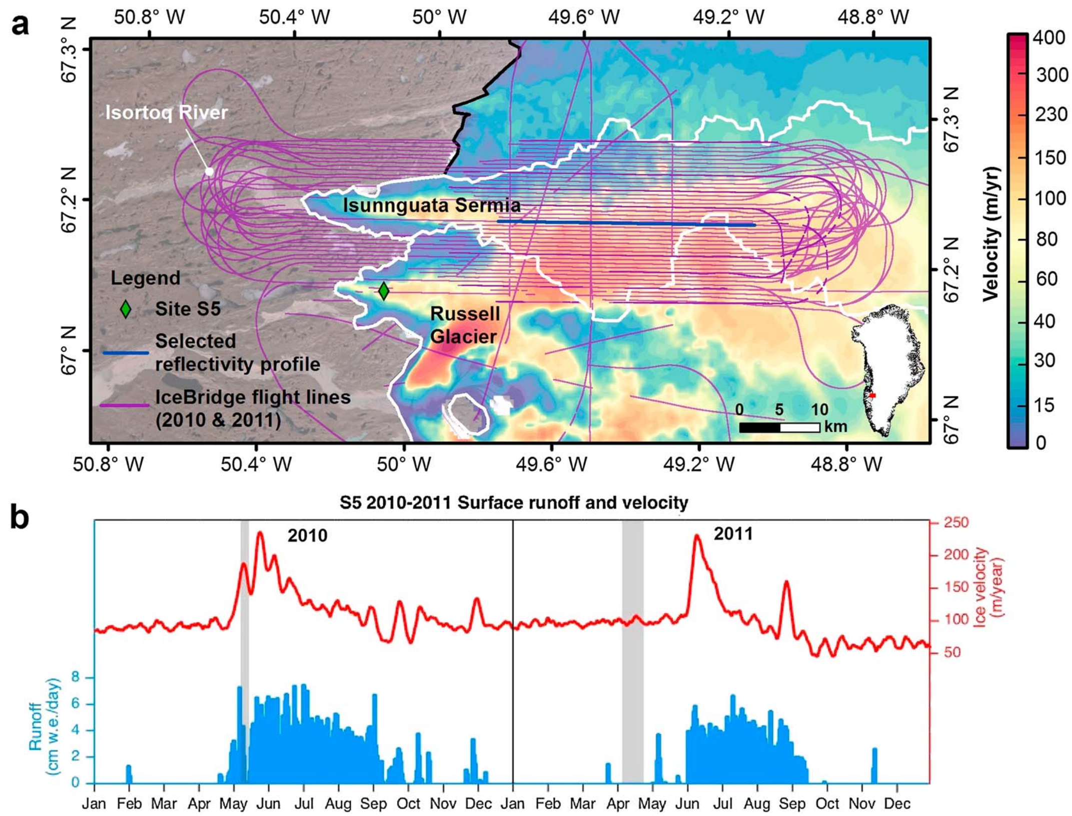

Figure 1. (a) Site setting with ice flow velocity from Advanced Land Observation Satellite (ALOS) and TerraSAR-X in winters of 2008 and 2009 [*Joughin et al.*, 2010]. IceBridge radar-sounding flight lines are shown as purple lines. The blue line indicates the location of the selected profile shown in Figure 2. (b) Velocity and surface runoff record from January 2010 to December 2011 at Site S5 along the K transect [*Van De Wal et al.*, 2015]. The gray bar represents the time period when the data were collected.

with the overlying ice compared to the surrounding bedrock [*Jacobel et al.*, 2009; *Matsuoka et al.*, 2012b; *Schroeder et al.*, 2016a]. Previous studies have suggested that thresholds ranging from 10 to 25 dB can be used to identify subglacial water bodies beneath ice sheets [*Dowdeswell and Siegert*, 2003; *Peters*, 2005; *Matsuoka*, 2011; *MacGregor et al.*, 2012; *Wolovick et al.*, 2013]. However, variations in englacial attenuation due to changes in ice temperature and chemical impurities can influence the basal echo intensity and interfere with the delineation of subglacial water bodies. Imaging subglacial water using radar reflectivities thus requires correcting for these variable attenuation losses.

2. Data and Methods

Here we apply a model-integrated method to correct for this variable attenuation loss and estimate basal reflectivity for Russell Glacier and Isunnguata Sermia (Russell-Isunnguata) in western Greenland. We apply this method to IceBridge Multichannel Coherent Radar Depth Sounder radar-sounding data from two seasons to examine changes in subglacial water distribution [*Gogineni et al.*, 2001] (see Text S1 in the supporting information). These data include nine profiles collected during the melt season of May 2010 when there was significant surface runoff (4–7 cm w.e. d^{-1}) and melt season ice flow speedup (~110% above the winter velocity; Figure 1). Additionally, we examine a high-resolution survey of the catchment acquired 11 months later in April 2011 at the end of winter before the onset of surface melting (Figure 1b).

We calculate basal reflectivity after correcting for the englacial attenuation, geometric spreading losses, and radar system variations between flights [*Jacobel et al.*, 2009; *Matsuoka et al.*, 2012a; *Wolovick et al.*, 2013; *Schroeder et al.*, 2016a] (see Text S2). To estimate the temperature-dependent attenuation rates, we use the temperature fields calculated using a three-dimensional steady state thermomechanical ice sheet model [*Morlighem et al.*, 2010; *Larour et al.*, 2012; *Seroussi et al.*, 2013] (see Text S3). The ice temperature field is then

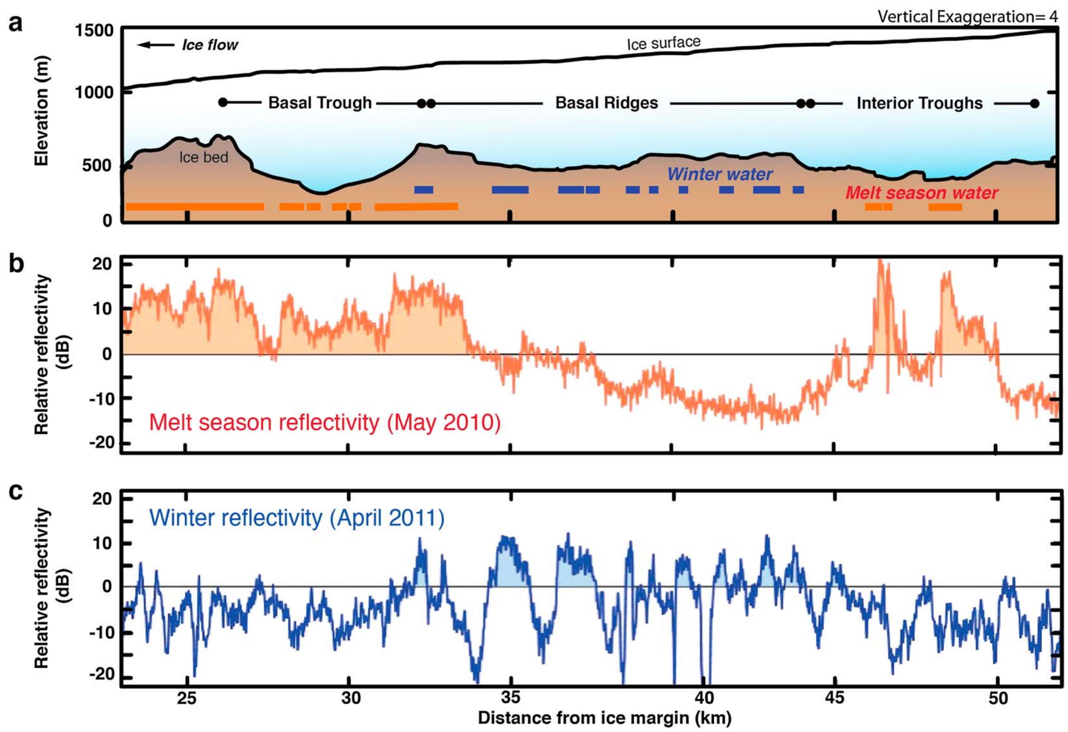

Figure 2. (a) Ice surface and bed elevation along a selected profile indicated by the blue line in Figure 1, where the 2010 and 2011 flight lines overlapped. The orange patches indicate the regions of winter subglacial water storage. The blue patches indicate the regions of melt season water distribution. (b) Melt season relative reflectivity profile collected on 15 May 2010. Relative reflectivities that exceed +9 dB from the zero line (i.e., 1 standard deviation from the mean) are interpreted as melt season water. (c) Winter relative reflectivity profile collected on 13 April 2011. Relative reflectivities that exceed +8 dB (i.e., 1 standard deviation from the mean) are interpreted as winter water.

used in a radar attenuation model [*MacGregor et al*., 2007] to estimate radar attenuation losses from temperature variations (see Text S4). We also estimate the attenuation losses due to the chemical impurities in the ice. The Russell/Isunnguata ice is primarily composed of Holocene chemistry [*MacGregor et al*., 2015b]. Therefore, we apply a uniform chemistry correction in the radar attenuation model and calculate basal reflectivities based on the Holocene impurity content [*MacGregor et al*., 2015a]. Following previous studies, we interpret high-reflectivity anomalies as subglacial water and lower values as relatively drier regions [e.g., *Jacobel et al*., 2009; *Wolovick et al*., 2013; *Schroeder et al*., 2016b].

3. Results

Differences in the reflectivity values for the melt season profiles and the winter survey show the seasonal changes of subglacial water distribution beneath Russell-Isunnguata (Figures 2 and 3). The 2010 melt season profile reveals two regions of high relative reflectivities separated by a more homogenous region of low relative reflectivity values (Figure 2b). The melt season reflectivity map shows that these higher relative reflectivity regions that are generally found in the sediment-filled troughs [*Dow et al*., 2013; *Mikkelsen et al*., 2013; *Lindbäck and Pettersson*, 2015] indicate widespread water, whereas the lower and more homogeneous reflectivities on the intervening bedrock ridges indicate a comparatively drained bed (Figure 3c).

Eleven months later, at the end of winter in April 2011, the reflectivity data capture a contrasting distribution of subglacial water. The range of the reflectivity is reduced, and the reflectivity attributes of the ridges and troughs are reversed. In the wintertime, the troughs are characterized by lower bed reflectivities, whereas the ridges have discontinuous patches of higher reflectivities (Figure 2c). These reflectivity characteristics are consistent throughout the 1500 km^2 area covered by the radar observations (Figure 3a). The high-reflectivity regions generally occur in areas with higher average bed elevation (200 to 470 m above sea level; Figure S10 in the supporting information). Both the single profile and the catchment map indicate that in the wintertime there is a substantial amount of subglacial water storage on the bedrock ridges compared to the troughs.

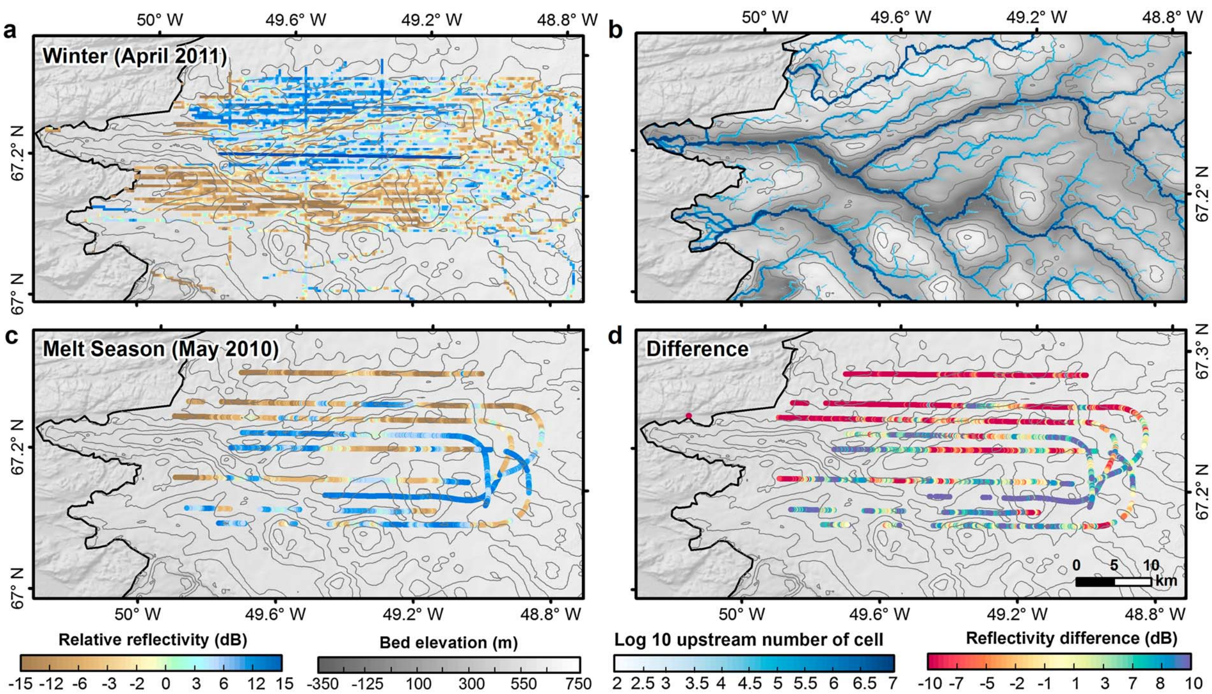

Figure 3. (a) Winter relative reflectivity map with 150 m bed contours. Higher reflectivity values are interpreted as the locations of subglacial water. (b) Bed topography with the same 150 m contours [*Morlighem et al*., 2014] and the calculated subglacial water flow accumulation from a routing analysis [*Chu et al*., 2016]. (c) Melt season relative reflectivity map with 150 m bed contours. (d) Difference of relative reflectivity between the melt season and winter maps. Positive differences indicate where the reflectivity is higher (wetter bed) in the melt season compared with the winter condition. The blue line in Figure 3a indicates the location of the selected profiles from 2010 and 2011, same line shown in Figure 2.

Notably, these winter storage regions are localized in areas with nearby flat hydraulic potential gradients ($<$9 Pa m^{-1}) that favor slow water flow and subglacial ponding (Figure 4). The storage also aligns with the smaller tributaries of our modeled hydrologic pathways, indicating that drainage was likely restricted along these smaller flow paths during the wintertime (Figure 3b). We identified more subglacial storage regions than the potential ponds calculated from a lower resolution hydraulic potential surface (150 m). Many small subglacial lakes, below the resolution of the hydraulic potential surface, may likely exist in this region.

This seasonal change in regional subglacial water distribution is captured where the two data sets overlap (Figure 3d). Two surveys, one in May 2010 and one in April 2011, have coincident geophysical survey lines. Positive differences show where the 2010 relative reflectivities exceed the 2011 values. The differences of +5 to 10 dB found along the basal troughs show increased meltwater drainage, whereas the negative differences ($-$5 to $-$10 dB) on the basal ridges indicate a relatively drained bed during the melt season.

4. Discussion

4.1. Control of Bed Properties on Subglacial Hydrology

The difference in reflectivity values across Isunnguata-Russell reveals the presence of wintertime subglacial water storage and provides a spatial context for subglacial water movement throughout the year. The presence of water storage primarily on the basal ridges where the ice is thin ($<$500 m), in contrast to the troughs with thicker ice ($>$800 m) and potentially higher basal melting, is surprising but arises from the low surface slope. The storage of water on topographic highs covered with relatively thin ice suggests that the material properties of glaciers bed, in addition to bed geometry, strongly influence subglacial water distribution.

The basal ridges are bedrock as shown by the high spectral roughness [*Lindbäck and Pettersson*, 2015]. The presence of wintertime water storage indicates that these bedrock ridges have relatively low hydraulic conductivity. The discontinuous wintertime reflectivity characteristics suggest the water bodies are isolated, likely in some form of linked cavities system (Figure 2c) [*Lliboutry*, 1968; *Walder*, 1986; *Bartholomaus et al*.,

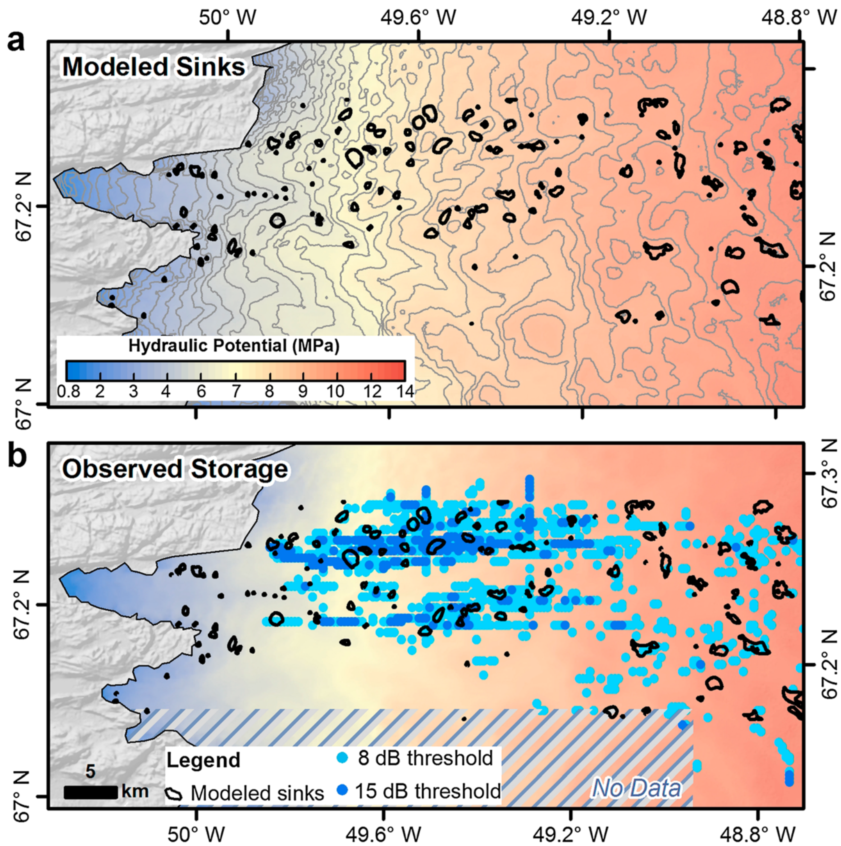

Figure 4. (a) Modeled hydraulic sinks with flat hydraulic potential gradients (black polygons) with contours of hydraulic potential of 2.5 MPa spacing. (b) Locations of observed winter water storage, defined by a high-reflectivity threshold of 1 standard deviation (+8 dB) (light blue dots) and 2 standard deviation (+15 dB) (dark blue dots). The black polygons are the modeled sinks shown in Figure 4a.

2011]. This cavity system isolates in the fall when the summer drainage conduits collapse viscously as effective pressures drop in response to lessening surface melt. Our interpretation is that these isolated, sealed water pockets are what the radar observed on bedrock ridges in the winter. During the melt season, the shift to a homogeneously lower reflectivity (Figure 2b) indicates increase in connectivity within these isolated systems as drainage pathways open or enlarge, allowing water to flow to the nearby active regions along the subglacial troughs [*Andrews et al.*, 2014].

In contrast, the subglacial troughs contain porous sediments as indicated by seismic evidence [*Booth et al.*, 2012; *Dow et al.*, 2013] and the low spectral roughness [*Lindbäck and Pettersson*, 2015]. As the summertime drainage system contracts during the fall and winter, water drains out of the ice-contact system while it closes [*Clarke*, 1987; *Iverson et al.*, 1995; *Flowers*, 2015]. Any remaining subglacial water then likely continues to seep through groundwater drainage, leaving little wintertime storage at the ice-bed interface. During the melt season, higher reflectivities localized in the troughs suggest that drainage is focused there once the upstream drainage system on the ridges connects to the troughs. An upstream supply of meltwater keeps the bed flooded, resulting in the specular, higher reflectivities that our analysis shows for the melt season.

4.2. Volume of Water Storage and Its Impact on Water Budget

Subglacial water storage is an integral part of the water budget in Greenland [*Rennermalm et al.*, 2012; *Van As et al.*, 2012; *Lindbäck et al.*, 2015; *Smith et al.*, 2015]. Previous studies at Isunnguata Sermia observed a large disagreement between the modeled runoff and the measured bulk proglacial discharge at Isortoq River [*Lindbäck et al.*, 2015; *Smith et al.*, 2015]. The missing volume of 1.8 to 2.7 km^3 has been attributed to either storage of subglacial water [*Smith et al*., 2015] or water piracy by Russell Glacier [*Lindbäck et al*., 2015]. We examine whether our observed storage could explain this missing volume. We use a high-reflectivity threshold of 1 standard deviation from the mean reflectivity to determine the maximum horizontal extent of the wintertime storage (Figure 4b). If all the missing water were stored in our observed winter storage area, water depths of 28–50 m (4–6% of the mean ice thickness) would be required. While subglacial water bodies deeper than 50 m are found in Antarctica [*Siegert*, 2005; *Smith et al*., 2009], it is unlikely that this volume of water is stored in our studied region. We did not observe a pronounced surface elevation change that would otherwise produced by the drainage of a 50 m subglacial lake. Therefore, the large, 50 m water depth required suggests that storage cannot solely explain the discrepancy in the water budget. A combination of storage and other processes, such as water piracy, groundwater losses, and supraglacial and englacial meltwater storage, are likely responsible for the missing water at Isunnguata Sermia [*Lindbäck et al*., 2015].

4.3. Impact of Storage on Early Season Velocity

We also examined the impact of subglacial water storage on the summer ice flow pattern at Russell-Isunnguata. Despite the similar surface melt forcing and topography configurations, previous studies show that the summer ice flow patterns vary considerably between Isunnguata Sermia and Russell Glacier [*Joughin et al*., 2010; *Palmer et al*., 2011; *Fitzpatrick et al*., 2013; *Lindbäck et al*., 2015]. Compared to Isunnguata Sermia, Russell Glacier has a more pronounced speedup in early summer and a stronger deceleration at the end of summer to below the wintertime values [*Lindbäck et al*., 2015; *Tedstone et al*., 2015]. The more pronounced speedup at Russell Glacier suggests that basal water pressure rises more rapidly in early summer than at Isunnguata Sermia [*Chandler et al*., 2013; *Cowton et al*., 2013; *Meierbachtol et al*., 2013]. This higher-pressure increase could be attributed to the greater variability in the rates of summertime supraglacial water drainage at Russell compared with Isunnguata [e.g., *Schoof*, 2010; *Palmer et al*., 2011]. In addition, any spatial variations in the state of the wintertime basal hydrologic system would also affect the rates of pressurization during the start of surface melting. The less pronounced early summer acceleration at Isunnguata Sermia could be associated with the widespread subglacial water storage that maintains elevated basal water pressures over the winter [*Clarke*, 2005; *Harper et al*., 2005; *Bartholomaus et al*., 2011; *Flowers*, 2015]. In contrast, the lack of substantial wintertime storage at Russell Glacier would result in a greater increase in basal water pressure at the start of the melt season and thus a more pronounced early summer speedup. Hence, we suggest that the individual catchment response to surface melting is determined by a combination of the subglacial hydrologic state at the start of the melt season as well as the variations in spring and summertime water input. The stronger late summer deceleration at Russell relative to Isunnguata indicates the formation of a focused, channelized subglacial drainage there [*Tedstone et al*., 2014], leading to efficient evacuation of basal meltwater at the end of summer. This is consistent with our radar results that indicate well-drained bed at the northern catchment of Russell in the wintertime. Together, our findings suggest that the spatial variations in subglacial topography, rates of surface meltwater input, and the subglacial water storage at the start of the melt season lead to differing glacier dynamic responses to surface melting across the Greenland Ice Sheet.

5. Conclusions

We present radar reflectivity analyses from two different seasons to understand the seasonal subglacial drainage development in Isunnguata Sermia and Russell Glacier. Our observations provide evidence of wintertime subglacial water storage in Isunnguata Sermia. This wintertime storage is primarily observed on bedrock ridges but not in subglacial troughs. In contrast, our reflectivity results in the melt season reveal the opposite drainage distribution with large amounts of water focused in the deep troughs but little observed on the ridges. This distinct seasonal drainage evolution suggests the material properties and the permeability of the glacier bed strongly influence the distribution of basal water. While the subglacial water storage we observed is widespread, this storage likely represents the tail end of the summer meltwater volume delivered to the bed from the ice surface. Furthermore, our findings suggest that the state of the subglacial hydrology at the onset of the melt season impacts the glacier dynamic response to surface melting in the early summer. Our study highlights the need for more detailed observations of how water moves subglacially throughout the year. Regional observations of meltwater distribution both on top of and beneath the ice sheet would help to improve assessment of changes in Greenland water budget in response to climate change.

Acknowledgments
W.C. is a recipient of the NASA Earth and Space Science Fellowship. D.M.S. is supported by a grant from the NASA Cryospheric Sciences Program. H.S. is supported by grants from the NASA Cryospheric Sciences and Sea Level Rise Programs. T.T.C and R.E.B are supported by grants from National Science Foundation (NSF) and NASA Cryospheric Sciences. S.P. is supported by the Natural Environment Research Council's Centre for Polar Observation. The radar data central to this work are provided by CReSIS from the University of Kansas. We thank Julienne Stroeve, Joseph MacGregor, and an anonymous referee for their constructive comments on this manuscript. We are grateful to Indrani Das, Jonathan Kingslake, Kirsty Tinto, and Timothy Bartholomaus for their suggestions for this work. Results produced in the paper are available upon request to the corresponding author. Radar data are available on the CReSIS data repository at https://data.cresis.ku.edu/data/rds/.

References

Alley, R. B., T. K. Dupont, B. R. Parizek, and S. Anandakrishnan (2005), Access of surface meltwater to beds of sub-freezing glaciers: Preliminary insights, *Ann. Glaciol.*, *40*(1), 8–14, doi:10.3189/172756405781813483.

Andrews, L. C., G. A. Catania, M. J. Hoffman, J. D. Gulley, M. P. Lüthi, C. Ryser, R. L. Hawley, and T. A. Neumann (2014), Direct observations of evolving subglacial drainage beneath the Greenland Ice Sheet, *Nature*, *514*(7520), 80–83, doi:10.1038/nature13796.

Aschwanden, A., E. Bueler, C. Khroulev, and H. Blatter (2012), An enthalpy formulation for glaciers and ice sheets, *J. Glaciol.*, *58*(209), 441–457, doi:10.3189/2012JoG11J088.

Bamber, J. L., et al. (2013), A new bed elevation dataset for Greenland, *Cryosphere*, *7*(2), 499–510, doi:10.5194/tc-7-499-2013.

Banwell, A. F., I. C. Willis, and N. S. Arnold (2013), Modeling subglacial water routing at Paakitsoq, W Greenland, *J. Geophys. Res. Earth Surf.*, *118*, 1282–1295, doi:10.1002/jgrf.20093.

Bartholomaus, T. C., R. S. Anderson, and S. P. Anderson (2011), Growth and collapse of the distributed subglacial hydrologic system of Kennicott Glacier, Alaska, USA, and its effects on basal motion, *J. Glaciol.*, *57*(206), 985–1002, doi:10.3189/002214311798843269.

Bartholomew, I., P. Nienow, A. Sole, D. Mair, T. Cowton, S. Palmer, and J. Wadham (2011), Supraglacial forcing of subglacial drainage in the ablation zone of the Greenland ice sheet, *Geophys. Res. Lett.*, *38*, L08502, doi:10.1029/2011GL047063.

Bartholomew, I., P. Nienow, A. Sole, D. Mair, T. Cowton, and M. A. King (2012), Short-term variability in Greenland Ice Sheet motion forced by time-varying meltwater drainage: Implications for the relationship between subglacial drainage system behavior and ice velocity, *J. Geophys. Res.*, *117*, F03002, doi:10.1029/2011JF002220.

Booth, A. D., R. A. Clark, B. Kulessa, T. Murray, J. Carter, S. Doyle, and A. Hubbard (2012), Thin-layer effects in glaciological seismic amplitude-versus-angle (AVA) analysis: Implications for characterising a subglacial till unit, Russell Glacier, West Greenland, *Cryosphere*, *6*, 909–922, doi:10.5194/tc-6-909-2012.

Carter, S. P., D. D. Blankenship, D. A. Young, and J. W. Holt (2009), Using radar-sounding data to identify the distribution and sources of subglacial water: Application to Dome C, East Antarctica, *J. Glaciol.*, *55*(194), 1025–1040, doi:10.3189/002214309790794931.

Chandler, D. M., et al. (2013), Evolution of the subglacial drainage system beneath the Greenland Ice Sheet revealed by tracers, *Nat. Geosci.*, *6*(3), 195–198, doi:10.1038/ngeo1737.

Chu, W., T. T. Creyts, and R. E. Bell (2016), Rerouting of subglacial water flow between neighboring glaciers in West Greenland, *J. Geophys. Res. Earth Surf.*, *121*, 925–938, doi:10.1002/2015JF003705.

Clarke, G. K. C. (1987), Subglacial till: A physical framework for its properties and processes, *J. Geophys. Res.*, *92*(B9), 9023, doi:10.1029/JB092iB09p09023.

Clarke, G. K. C. (2005), Subglacial processes, *Annu. Rev. Earth Planet. Sci.*, *33*(1), 247–276, doi:10.1146/annurev.earth.33.092203.122621.

Cowton, T., P. Nienow, A. Sole, J. Wadham, G. Lis, I. Bartholomew, D. Mair, and D. Chandler (2013), Evolution of drainage system morphology at a land-terminating Greenlandic outlet glacier, *J. Geophys. Res. Earth Surf.*, *118*, 29–41, doi:10.1029/2012JF002540.

Cuffey, K., and W. S. Paterson (2010), *The Physics of Glaciers*, 4th ed., Butterworth-Heinemann/Elsevier, Oxford, U. K.

Das, S. B., I. Joughin, M. D. Behn, I. M. Howat, M. A. King, D. Lizarralde, and M. P. Bhatia (2008), Fracture propagation to the base of the Greenland Ice Sheet during supraglacial lake drainage, *Science*, *320*(5877), 778–781, doi:10.1126/science.1153360.

Dow, C. F., A. Hubbard, A. D. Booth, S. H. Doyle, A. Gusmeroli, and B. Kulessa (2013), Seismic evidence of mechanically weak sediments underlying Russell Glacier, West Greenland, *Ann. Glaciol.*, *54*(64), 135–141, doi:10.3189/2013AoG64A032.

Dowdeswell, J. A., and M. J. Siegert (2003), The physiography of modern Antarctic subglacial lakes, *Global Planet. Change*, *35*(3–4), 221–236, doi:10.1016/S0921-8181(02)00128-5.

Fitzpatrick, A. A. W., A. Hubbard, I. Joughin, D. J. Quincey, D. Van As, A. P. B. Mikkelsen, S. H. Doyle, B. Hasholt, and G. A. Jones (2013), Ice flow dynamics and surface meltwater flux at a land-terminating sector of the Greenland Ice Sheet, *J. Glaciol.*, *59*(216), 687–696, doi:10.3189/2013JoG12J143.

Flowers, G. E. (2015), Modelling water flow under glaciers and ice sheets, *Proc. R. Soc. A Math. Phys. Eng. Sci.*, *471*(2176, 20140907), doi:10.1098/rspa.2014.0907.

Forster, R. R., et al. (2013), Extensive liquid meltwater storage in firn within the Greenland Ice Sheet, *Nat. Geosci.*, 1–4, doi:10.1038/ngeo2043.

Gadallah, M. R., and R. Fisher (2009), *Exploration Geophysics*, Springer, Berlin Heidelberg.

Gogineni, S., D. Tammana, J. Stiles, C. Allen, and K. Jezek (2001), Coherent radar ice thickness measurements over the Greenland Ice Sheet, *J. Geophys. Res.*, *106*(D24), 33, 761–33,772, doi:10.1029/2001JD900183.

Harper, J. T., N. F. Humphrey, W. T. Pfeffer, T. Fudge, and S. O. Neel (2005), Evolution of subglacial water pressure along a glacier's length, *Ann. Glaciol.*, *40*(1981), 31–36.

Harrington, J. A., N. F. Humphrey, and J. T. Harper (2015), Temperature distribution and thermal anomalies along a flowline of the Greenland Ice Sheet, *Ann. Glaciol.*, *56*(70), 98–104, doi:10.3189/2015AoG70A945.

Hewitt, I. J. (2013), Seasonal changes in ice sheet motion due to melt water lubrication, *Earth Planet. Sci. Lett.*, *371–372*, 16–25, doi:10.1016/j.epsl.2013.04.022.

Iken, A., and R. A. Bindschadler (1986), Combined measurements of subglacial water pressure and surface velocity at Findelengletscher, Switzerland, conclusions about drainage system and sliding mechanism, *J. Glaciol.*, *32*, 101–119.

Iverson, N. R., B. Hanson, R. L. Hooke, and P. Jansson (1995), Flow mechanism of glaciers on soft beds, *Science*, *267*(5194), 80–1, doi:10.1126/science.267.5194.80.

Jacobel, R. W., B. C. Welch, D. Osterhouse, R. Pettersson, and J. A. MacGregor (2009), Spatial variation of radar-derived basal conditions on Kamb Ice Stream, West Antarctica, *Ann. Glaciol.*, *50*(51), 10–16, doi:10.3189/172756409789097504.

Joughin, I., B. E. Smith, I. M. Howat, T. Scambos, and T. Moon (2010), Greenland flow variability from ice-sheet-wide velocity mapping, *J. Glaciol.*, *56*(197), 415–430, doi:10.3189/002214310792447734.

Joughin, I., S. B. Das, G. E. Flowers, M. D. Behn, R. B. Alley, M. A. King, B. E. Smith, J. L. Bamber, M. R. van den Broeke, and J. H. van Angelen (2013), Influence of ice-sheet geometry and supraglacial lakes on seasonal ice-flow variability, *Cryosphere*, *7*(4), 1185–1192, doi:10.5194/tc-7-1185-2013.

Kleiner, T., M. Rückamp, J. H. Bondzio, and A. Humbert (2015), Enthalpy benchmark experiments for numerical ice sheet models, *Cryosphere*, *9*(1), 217–228, doi:10.5194/tc-9-217-2015.

Langley, K., J. Kohler, K. Matsuoka, A. Sinisalo, T. Scambos, T. Neumann, A. Muto, J. G. Winther, and M. Albert (2011), Recovery Lakes, East Antarctica: Radar assessment of sub-glacial water extent, *Geophys. Res. Lett.*, *38*, L05501, doi:10.1029/2010GL046094.

Larour, E., H. Seroussi, M. Morlighem, and E. Rignot (2012), Continental scale, high order, high spatial resolution, ice sheet modeling using the Ice Sheet System Model (ISSM), *J. Geophys. Res.*, *117*, F01022, doi:10.1029/2011JF002140.

Lindbäck, K., and R. Pettersson (2015), Spectral roughness and glacial erosion of a land-terminating section of the Greenland Ice Sheet, *Geomorphology*, *238*, 149–159, doi:10.1016/j.geomorph.2015.02.027.

Lindbäck, K., R. Pettersson, A. L. Hubbard, S. H. Doyle, D. van As, A. B. Mikkelsen, and A. A. Fitzpatrick (2015), Subglacial water drainage, storage, and piracy beneath the Greenland Ice Sheet, *Geophys. Res. Lett.*, *42*, 7606–7614, doi:10.1002/2015GL065393.

Lliboutry, L. (1968), General theory of subglacial cavitation and sliding of temperate glaciers, *J. Glaciol.*, *7*(49), 21–58.

MacGregor, J. A., D. P. Winebrenner, H. Conway, K. Matsuoka, P. A. Mayewski, and G. D. Clow (2007), Modeling englacial radar attenuation at Siple Dome, West Antarctica, using ice chemistry and temperature data, *J. Geophys. Res.*, *112*, F03008, doi:10.1029/2006JF000717.

MacGregor, J. A., K. Matsuoka, E. D. Waddington, D. P. Winebrenner, and F. Pattyn (2012), Spatial variation of englacial radar attenuation: Modeling approach and application to the Vostok flowline, *J. Geophys. Res.*, *117*, F03022, doi:10.1029/2011JF002327.

MacGregor, J. A., et al. (2015a), Radar attenuation and temperature within the Greenland Ice Sheet, *J. Geophys. Res. Earth Surf.*, *120*, 983–1008, doi:10.1002/2014JF003418.

MacGregor, J. A., M. A. Fahnestock, G. A. Catania, J. D. Paden, S. Prasad Gogineni, S. K. Young, S. C. Rybarski, A. N. Mabrey, B. M. Wagman, and M. Morlighem (2015b), Radiostratigraphy and age structure of the Greenland Ice Sheet, *J. Geophys. Res. Earth Surf.*, *120*, 212–241, doi:10.1002/2014JF003215.

Mandea, M., and M. Korte (2011), *Geomagnetic Observations and Models*, edited by M. Mandea and M. Korte, Springer, Dordrecht, Netherlands.

Matsuoka, K. (2011), Pitfalls in radar diagnosis of ice-sheet bed conditions: Lessons from englacial attenuation models, *Geophys. Res. Lett.*, *38*, L05505, doi:10.1029/2010GL046205.

Matsuoka, K., J. A. MacGregor, and F. Pattyn (2012a), Predicting radar attenuation within the Antarctic ice sheet, *Earth Planet. Sci. Lett.*, *359–360*, 173–183, doi:10.1016/j.epsl.2012.10.018.

Matsuoka, K., F. Pattyn, D. Callens, and H. Conway (2012b), Radar characterization of the basal interface across the grounding zone of an ice-rise promontory in East Antarctica, *Ann. Glaciol.*, *53*(60), 29–34, doi:10.3189/2012AoG60A106.

McMillan, M., P. Nienow, A. Shepherd, T. Benham, and A. Sole (2007), Seasonal evolution of supra-glacial lakes on the Greenland Ice Sheet, *Earth Planet. Sci. Lett.*, *262*(3–4), 484–492, doi:10.1016/j.epsl.2007.08.002.

Meierbachtol, T., J. Harper, and N. Humphrey (2013), Basal drainage system response to increasing surface melt on the Greenland Ice Sheet, *Science*, *341*(6147), 777–9, doi:10.1126/science.1235905.

Mikkelsen, A. B., B. Hasholt, N. T. Knudsen, and M. H. Nielsen (2013), Jokulhlaups and sediment transport in Watson River, Kangerlussuaq, West Greenland, *Hydrol. Res.*, *44*(1), 58–67, doi:10.2166/nh.2012.165.

Moon, T., I. Joughin, B. Smith, M. R. van den Broeke, W. J. van de Berg, B. Noël, and M. Usher (2014), Distinct patterns of seasonal Greenland glacier velocity, *Geophys. Res. Lett.*, *41*, 7209–7216, doi:10.1002/2014GL061836.

Morlighem, M., E. Rignot, H. Seroussi, E. Larour, H. Ben Dhia, and D. Aubry (2010), Spatial patterns of basal drag inferred using control methods from a full-Stokes and simpler models for Pine Island Glacier, West Antarctica, *Geophys. Res. Lett.*, *37*, L14502, doi:10.1029/2010GL043853.

Morlighem, M., E. Rignot, J. Mouginot, H. Seroussi, and E. Larour (2014), Deeply incised submarine glacial valleys beneath the Greenland Ice Sheet, *Nat. Geosci.*, *7*(6), 418–422, doi:10.1038/ngeo2167.

Noël, B., W. J. van de Berg, E. van Meijgaard, P. Kuipers Munneke, R. S. W. van de Wal, and M. R. van den Broeke (2015), Evaluation of the updated regional climate model RACMO2.3: Summer snowfall impact on the Greenland Ice Sheet, *Cryosphere*, *9*(5), 1831–1844, doi:10.5194/tc-9-1831-2015.

Palmer, S., A. Shepherd, P. Nienow, and I. Joughin (2011), Seasonal speedup of the Greenland Ice Sheet linked to routing of surface water, *Earth Planet. Sci. Lett.*, *302*(3–4), 423–428, doi:10.1016/j.epsl.2010.12.037.

Peters, M. E. (2005), Analysis techniques for coherent airborne radar sounding: Application to West Antarctic ice streams, *J. Geophys. Res.*, *110*, B06303, doi:10.1029/2004JB003222.

Phillips, T., H. Rajaram, and K. Steffen (2010), Cryo-hydrologic warming: A potential mechanism for rapid thermal response of ice sheets, *Geophys. Res. Lett.*, *37*, L20503, doi:10.1029/2010GL044397.

Rennermalm, A. K., L. C. Smith, V. W. Chu, R. R. Forster, J. E. Box, and B. Hagedorn (2012), Proglacial river stage, discharge, and temperature datasets from the Akuliarusiarsuup Kuua River northern tributary, Southwest Greenland, 2008–2011, *Earth Syst. Sci. Data*, *4*(1), 1–12, doi:10.5194/essd-4-1-2012.

Rignot, E., and P. Kanagaratnam (2006), Changes in the velocity structure of the Greenland Ice Sheet, *Science*, *311*(5763), 986–90, doi:10.1126/science.1121381.

Schoof, C. (2005), The effect of cavitation on glacier sliding, *Proc. R. Soc. A Math. Phys. Eng. Sci.*, *461*(2055), 609–627, doi:10.1098/rspa.2004.1350.

Schoof, C. (2010), Ice-sheet acceleration driven by melt supply variability, *Nature*, *468*(7325), 803–6, doi:10.1038/nature09618.

Schroeder, D., C. Grima, and D. Blankenship (2016a), Evidence for variable grounding-zone and shear-margin basal conditions across Thwaites Glacier, West Antarctica, *Geophysics*, *81*(1), WA35–WA43, doi:10.1190/geo2015-0122.1.

Schroeder, D. M., H. Seroussi, W. Chu, and D. A. Young (2016b), Adaptively constraining radar attenuation and temperature across the Thwaites Glacier catchment using bed echoes, *J. Glaciol.*, 1–8, doi:10.1017/jog.2016.100.

Seroussi, H., M. Morlighem, E. Rignot, A. Khazendar, E. Larour, and J. Mouginot (2013), Dependence of century-scale projections of the Greenland Ice Sheet on its thermal regime, *J. Glaciol.*, *59*(218), 1024–1034, doi:10.3189/2013JoG13J054.

Shapiro, N. M., and M. H. Ritzwoller (2004), Inferring surface heat flux distributions guided by a global seismic model: Particular application to Antarctica, *Earth Planet. Sci. Lett.*, *223*(1–2), 213–224, doi:10.1016/j.epsl.2004.04.011.

Shreve, R. (1972), Movement of water in glaciers, *J. Glaciol.*, *11*(62), 205–14.

Siegert, M. J. (2005), Lakes beneath the ice sheet: The occurrence, analysis, and future exploration of Lake Vostok and other Antarctic subglacial lakes, *Annu. Rev. Earth Planet. Sci.*, *33*(1), 215–245, doi:10.1146/annurev.earth.33.092203.122725.

Smith, B. E., H. A. Fricker, I. R. Joughin, and S. Tulaczyk (2009), An inventory of active subglacial lakes in Antarctica detected by ICESat (2003–2008), *J. Glaciol.*, *55*(192), 573–595, doi:10.3189/002214309789470879.

Smith, L. C., et al. (2015), Efficient meltwater drainage through supraglacial streams and rivers on the southwest Greenland Ice Sheet, *Proc. Natl. Acad. Sci. U.S.A.*, *112*(4), 1001–1006, doi:10.1073/pnas.1413024112.

Sole, A., P. Nienow, I. Bartholomew, D. Mair, T. Cowton, A. Tedstone, and M. A. King (2013), Winter motion mediates dynamic response of the Greenland Ice Sheet to warmer summers, *Geophys. Res. Lett.*, *40*, 3940–3944, doi:10.1002/grl.50764.

Sundal, A. V., A. Shepherd, P. Nienow, E. Hanna, S. Palmer, and P. Huybrechts (2011), Melt-induced speed-up of Greenland Ice Sheet offset by efficient subglacial drainage, *Nature*, *469*(7331), 521–4, doi:10.1038/nature09740.

Tarboton, D. G. (1997), A new method for the determination of flow directions and upslope areas in grid digital elevation models, *Water Resour. Res.*, *33*(2), 309–319, doi:10.1029/96WR03137.

Tedstone, A. J., P. W. Nienow, A. J. Sole, D. W. F. Mair, T. R. Cowton, I. D. Bartholomew, and M. A. King (2013), Greenland Ice Sheet motion insensitive to exceptional meltwater forcing, *Proc. Natl. Acad. Sci. U.S.A.*, *110*(49), 19,719–19,724, doi:10.1073/pnas.1315843110.

Tedstone, A. J., P. W. Nienow, N. Gourmelen, and A. J. Sole (2014), Greenland Ice Sheet annual motion insensitive to spatial variations in subglacial hydraulic structure, *Geophyss. Res. Lett.*, *41*, 8910–8917, doi:10.1002/2014GL062386.

Tedstone, A. J., P. W. Nienow, N. Gourmelen, A. Dehecq, D. Goldberg, and E. Hanna (2015), Decadal slowdown of a land-terminating sector of the Greenland Ice Sheet despite warming, *Nature*, *526*(7575), 692–695, doi:10.1038/nature15722.

Van As, D., A. L. Hubbard, B. Hasholt, A. B. Mikkelsen, M. R. Van Den Broeke, and R. S. Fausto (2012), Large surface meltwater discharge from the Kangerlussuaq sector of the Greenland Ice Sheet during the record-warm year 2010 explained by detailed energy balance observations, *Cryosphere*, *6*(1), 199–209, doi:10.5194/tc-6-199-2012.

Van De Wal, R. S. W., et al. (2015), Self-regulation of ice flow varies across the ablation area in south-west Greenland, *Cryosphere*, *9*(2), 603–611, doi:10.5194/tc-9-603-2015.

van den Broeke, M., J. Bamber, J. Ettema, E. Rignot, E. Schrama, W. J. van de Berg, E. van Meijgaard, I. Velicogna, and B. Wouters (2009), Partitioning recent Greenland mass loss, *Science*, *326*(5955), 984–6, doi:10.1126/science.1178176.

Walder, J. S. (1986), Hydraulics of subglacial cavities, *J. Glaciol.*, *32*(112), 439–445.

Wolovick, M. J., R. E. Bell, T. T. Creyts, and N. Frearson (2013), Identification and control of subglacial water networks under Dome A, Antarctica, *J. Geophys. Res. Earth Surf.*, *118*, 140–154, doi:10.1029/2012JF002555.

Zwally, H. J., W. Abdalati, T. Herring, K. Larson, J. Saba, and K. Steffen (2002), Surface melt-induced acceleration of Greenland ice-sheet flow, *Science*, *297*(5579), 218–22, doi:10.1126/science.1072708.